

## Electronic structure of $K_3Ba_3C_{60}$ and $Rb_3Ba_3C_{60}$ superconductors

Koichiro Umemoto and Susumu Saito

*Department of Physics, Tokyo Institute of Technology, 2-12-1 Oh-okayama, Meguro-ku, Tokyo 152-8551, Japan*

Atsushi Oshiyama

*Institute of Physics, University of Tsukuba, Tennodai, Tsukuba 305-8571, Japan*

(Received 11 May 1999; revised manuscript received 28 July 1999)

We have studied the electronic structure of the superconducting fullerides  $K_3Ba_3C_{60}$  and  $Rb_3Ba_3C_{60}$  using the local-density approximation in the density functional theory. Their conduction-band profiles are found to be quantitatively very similar to each other although the lattice constant of  $K_3Ba_3C_{60}$  is definitely smaller than that of  $Rb_3Ba_3C_{60}$ . The density of states at Fermi level of  $K_3Ba_3C_{60}$  is slightly larger than that of  $Rb_3Ba_3C_{60}$ . In addition,  $C_{60}$  states are found to be hybridized not only with Ba states but also with K (Rb) states. These results are in sharp contrast to  $A_3C_{60}$  superconductors ( $A=K$  and  $Rb$ ). The hybridization is expected to play an important role in their superconducting properties since carriers are found to be not only on  $C_{60}$  but also around K (Rb) sites as well as Ba sites. [S0163-1829(99)07747-4]

### I. INTRODUCTION

Ever since the discovery of superconductivity in the potassium-doped fulleride,<sup>1</sup> many experimental and theoretical studies of superconducting alkali-doped fullerides have been carried out.<sup>2-12</sup> The superconducting phase has been identified to be the face-centered cubic (fcc)  $A_3C_{60}$ .<sup>2</sup> In these fcc  $A_3C_{60}$ , interestingly, the larger the lattice constant is, the higher the superconducting transition temperature ( $T_c$ ) is.<sup>3</sup> That is, K or heavier alkali atoms doped at interstitial sites of the close-packed fcc  $C_{60}$  lattice are large enough to expand the lattice constant and doping larger alkali atoms gives rise to the increase of  $T_c$ , e.g., 29 K in  $Rb_3C_{60}$ <sup>4</sup> versus 19 K in  $K_3C_{60}$ .<sup>5</sup> Accordingly,  $Cs_2RbC_{60}$  has the highest  $T_c$  (33 K) among fcc  $A_3C_{60}$  superconductors.<sup>6</sup> This monotonical relation between the lattice constant and  $T_c$  can be, at least qualitatively, explained by the standard BCS-type theory based on their electronic structure.<sup>7-11</sup> The increase of their lattice constant makes the interaction between  $C_{60}$ s weaker, the half-filled  $t_{1u}$  band (originating from the  $t_{1u}$  state, the so-called LUMO, the lowest unoccupied molecular orbital, of the  $C_{60}$  cluster) less dispersive, the density of states at the Fermi level [ $N(E_F)$ ] larger, and consequently their  $T_c$  higher according to the BCS-type theory. Pressure dependence of  $T_c$  in  $Rb_3C_{60}$  is also consistent with the alkali-element dependence of  $T_c$  in  $A_3C_{60}$ . Its  $T_c$  decreases as its lattice constant is shortened by applying pressure.<sup>12</sup> Therefore, in  $A_3C_{60}$  superconductors, a rather universal relationship between the lattice constant and  $T_c$  holds regardless of the way of varying the lattice constant.

On the other hand, body-centered cubic (bcc)  $A_3Ba_3C_{60}$  superconductors ( $A=K, Rb$ , or their mixture) synthesized recently are found to show a complex relationship between the lattice constant and  $T_c$  which is different from that of  $A_3C_{60}$ .<sup>13-15</sup>  $T_c$  of  $K_3Ba_3C_{60}$  is 5.6 K which is higher than that of  $Rb_3Ba_3C_{60}$  (2.0 K), although the latter has the larger lattice constant than the former. However, the decrease of the lattice constant by applying pressure in  $K_3Ba_3C_{60}$  is found to

result in the lower  $T_c$ . In the case of similar alkaline-earth-doped bcc fullerides,  $Sr_6C_{60}$  and  $Ba_6C_{60}$ ,<sup>16,17</sup> it has been shown that  $C_{60}$  states are hybridized strongly with the alkaline-earth metal  $d$  states. This hybridization gives rise to the overlap between valence and conduction bands and makes these fullerides semimetallic.<sup>18,19</sup> Moreover,  $Sr_6C_{60}$  and  $Ba_6C_{60}$  are different from each other in the details of their band structure around  $E_F$  and consequently  $N(E_F)$  of  $Sr_6C_{60}$  is higher than that of  $Ba_6C_{60}$ , although the lattice constant of  $Sr_6C_{60}$  is smaller than that of  $Ba_6C_{60}$ . Their metallic behavior and  $N(E_F)$  values have been recently confirmed experimentally.<sup>20</sup> Therefore, also in  $A_3Ba_3C_{60}$ , the hybridization between  $C_{60}$  states and Ba states may play an important role in their electronic properties.

In this paper, to clarify the details of the hybridization and their electronic properties, we study the electronic structure of  $K_3Ba_3C_{60}$  and  $Rb_3Ba_3C_{60}$  in the framework of the density functional theory. The hybridization is found to be present not only between Ba and  $C_{60}$  states but also between K and  $C_{60}$  states. The band structure of  $K_3Ba_3C_{60}$  is very similar to that of  $Rb_3Ba_3C_{60}$  although the lattice constant of  $K_3Ba_3C_{60}$  ( $a=11.246$  Å) is smaller than that of  $Rb_3Ba_3C_{60}$  ( $a=11.32$  Å). From the comparative study of several hypothetical bcc solid  $C_{60}$ , i.e., the pristine  $C_{60}$ , bcc  $K_3C_{60}$ , and  $Ba_3C_{60}$ , it is found that  $C_{60}$  states are hybridized with alkali and Ba states and that the  $t_{1g}$ -derived band (originating from the  $t_{1g}$  state, the second LUMO of the  $C_{60}$  cluster) is half filled in  $A_3Ba_3C_{60}$ . Owing to this hybridization,  $N(E_F)$  of  $K_3Ba_3C_{60}$  obtained is slightly larger than that of  $Rb_3Ba_3C_{60}$ , which is qualitatively consistent with the higher  $T_c$  in  $K_3Ba_3C_{60}$ . This hybridization should have an important effect on their electronic transport properties since carriers are distributed around alkali and Ba sites as well as on  $C_{60}$  due to the hybridization. In addition, we have also studied  $K_6C_{60}$  and its hypothetical pristine phase comparatively and confirmed the existence of hybridization between K and  $C_{60}$  states in  $K_6C_{60}$  as well.

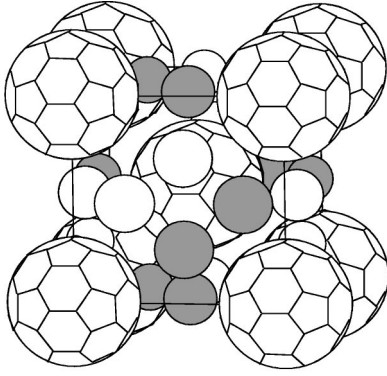


FIG. 1. Structure of  $K_3Ba_3C_{60}$  studied in the present work. Shaded and white spheres denote K and Ba atoms, respectively.

## II. COMPUTATIONAL METHOD

In the electronic-structure calculations, we use the local-density approximation (LDA) within the framework of the density functional theory.<sup>21,22</sup> We adopt the Ceperley-Alder exchange-correlation potential in the LDA.<sup>23</sup> The norm-conserving pseudopotentials<sup>24</sup> with the Kleinman-Bylander separable approximation<sup>25</sup> are also adopted. The real-space partition method<sup>26</sup> is used in order to avoid the breakdown of the separable approximation for K, Rb, and Ba. A plane-wave basis set with a cutoff energy of 50 Ry is used.

In  $A_3Ba_3C_{60}$  to be studied, A and Ba atoms are experimentally reported to be randomly located at interstitial sites of the bcc lattice of  $C_{60}$  in which all  $C_{60}$  clusters are orientationally ordered with the highest-symmetry orientation as in the case of  $K_6C_{60}$  and  $Ba_6C_{60}$ . In order to perform the electronic-structure calculation, we assume the fixed location of A and Ba atoms shown in Fig. 1, which realizes the highest-possible symmetry ( $C_3$  point group) under the condition that the unit cell contains one  $C_{60}$  cluster. Although even higher point-group symmetry  $T_h$  can be assigned to the actual  $A_3Ba_3C_{60}$  materials owing to the averaging from the random occupancy, the effect of lowering the symmetry from  $T_h$  to  $C_3$  to their band structure is confirmed to be very small as will be shown in the next section. In  $K_3Ba_3C_{60}$ , atomic coordinates determined experimentally<sup>13</sup> are used. As

for  $Rb_3Ba_3C_{60}$  of which atomic coordinates have not been reported experimentally, we have optimized the geometry by using the conjugate-gradient procedure<sup>27</sup> under the reported lattice constant of 11.32 Å. Optimized atomic coordinates of Rb and Ba atoms in  $Rb_3Ba_3C_{60}$  are (0.0, 0.5, 0.2817) and (0.0, 0.5, -0.2816), respectively. These coordinates are very close to those of K and Ba atoms in  $K_3Ba_3C_{60}$ ,<sup>13</sup> (0.0, 0.5, 0.2798) and its symmetry-related coordinates, respectively.

In alkali-metal atoms, it is known that there is considerable spatial overlap between valence states and the highest-energy core  $p$  states.<sup>28</sup> In order to clarify the effect of this overlap, we have performed the electronic-structure calculation on  $K_3Ba_3C_{60}$  with treating K  $3p$  and Ba  $5p$  states as valence states. It has been confirmed that their treatment as either valence or core states leads to the same conclusion although there are small quantitative differences in the band structure.

## III. RESULTS AND DISCUSSION

Valence-electron densities of  $K_3Ba_3C_{60}$  and the pristine  $C_{60}$  obtained are shown in Figs. 2(a) and 2(b). Also the positive-value region of their difference is shown together [Fig. 2(c)] in order to visualize the spatial distribution of the additional electrons introduced via doping. The lattice constant of this pristine bcc  $C_{60}$  assumed is identical to that of  $K_3Ba_3C_{60}$ . Interestingly, Figure 2(c) indicates that there remain considerable electron densities around not only Ba but also K sites and that the charge transfer from neither K nor Ba atom to  $C_{60}$  is complete. This implies that  $C_{60}$  states may be hybridized with K states as well as with Ba states. We have also calculated the valence-electron density of  $Rb_3Ba_3C_{60}$  which is found to be very similar to that of  $K_3Ba_3C_{60}$ . Therefore, also in  $Rb_3Ba_3C_{60}$ ,  $C_{60}$  states may be hybridized with Rb and Ba states.

In Fig. 3, the band structure of  $K_3Ba_3C_{60}$  and density of states (DOS) of  $K_3Ba_3C_{60}$  obtained are shown. The band structure of  $K_3Ba_3C_{60}$  is, as will be discussed later, more dispersive than that of the pristine bcc  $C_{60}$  having the same lattice constant as that of  $K_3Ba_3C_{60}$ . It is also the case in  $Rb_3Ba_3C_{60}$ . This band broadening clearly

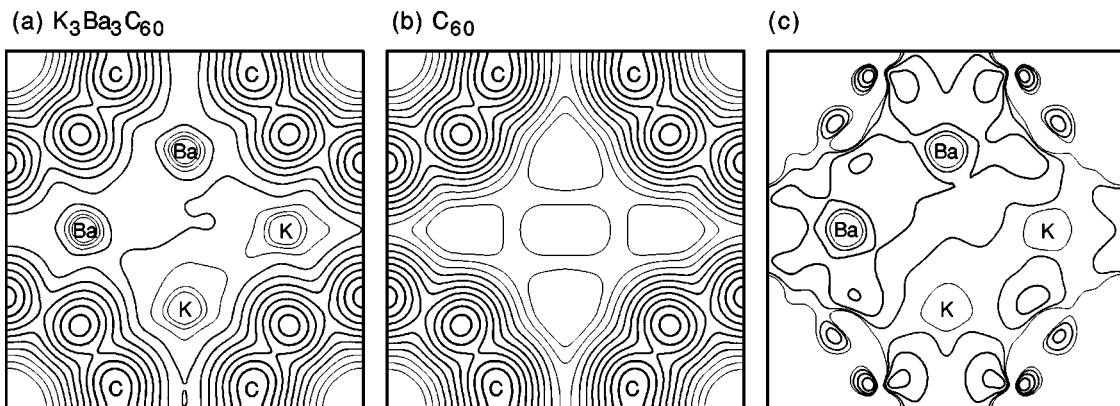


FIG. 2. (a) Valence electron density on the (100) plane of  $K_3Ba_3C_{60}$ , (b) that of the pristine  $C_{60}$ , and (c) the difference between  $K_3Ba_3C_{60}$  and the pristine bcc  $C_{60}$  valence-electron densities [ $[(a)-(b)]$ ]. In (c), positive-value regions are shown. The center of the  $C_{60}$  cluster is located at each corner. Each contour line indicates twice (half) the density of the neighboring thinner (thicker) contour lines. In (a) and (b), the highest-density contour lines correspond to 0.2 in atomic units. These lines, shown by the thickest lines, appear around the C atoms and the C-C bonds. In (c), the highest density contour lines correspond to 0.00625.

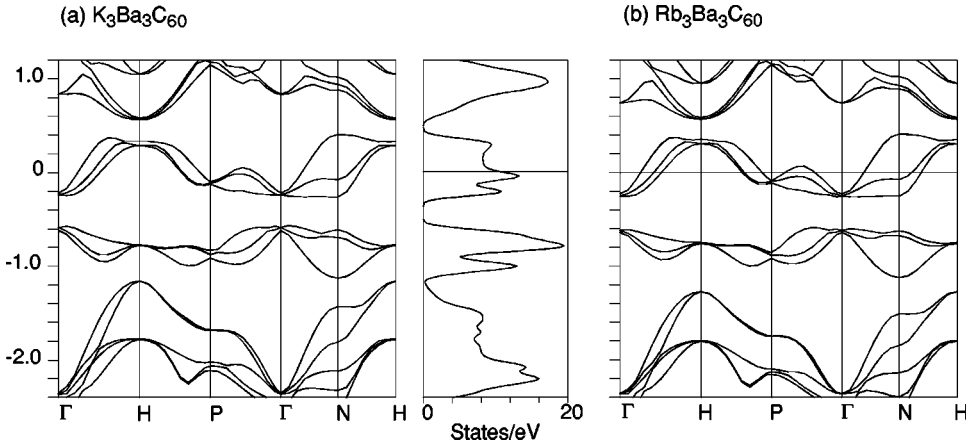


FIG. 3. (a) The band structure (square panel) and the density of states (rectangular panel) of (a)  $\text{K}_3\text{Ba}_3\text{C}_{60}$  and (b) the band structure of  $\text{Rb}_3\text{Ba}_3\text{C}_{60}$ . Energy is measured from the Fermi level denoted by the horizontal line. The band where the Fermi level lies is the  $t_{1g}$ -derived band. The density of states is broadened by using the Gaussian-distribution function with the width of 0.001 eV.

indicates the presence of the hybridization between  $\text{C}_{60}$  states and alkali and Ba states mentioned above. We call the hybridized band of  $\text{C}_{60}$ - $t_{1g}$ , alkali, and Ba states hereafter “ $t_{1g}$  band” for the sake of simplicity.

In the system that has the  $T_h$ -point-group symmetry, three branches of the  $t_{1g}$  band should be degenerate at the  $\Gamma$  point. Because the system we study has the  $C_3$ -point-group symmetry, the degeneracy of the  $t_{1g}$  band at the  $\Gamma$  point are now slightly lifted. However, three eigenvalues of the  $t_{1g}$  band at the  $\Gamma$  point are still within a very small energy range (0.02 eV). Therefore, the effect of lowering the symmetry from  $T_h$  to  $C_3$  to their band structure is confirmed to be very small. Unlike  $\text{Ba}_6\text{C}_{60}$ ,<sup>18,19</sup> the  $t_{1g}$  band is separated completely from the higher conduction band. The Fermi level lies in the  $t_{1g}$  band, which is half filled. Surprisingly, not only the shapes but also  $t_{1g}$ -band widths of  $\text{K}_3\text{Ba}_3\text{C}_{60}$  and  $\text{Rb}_3\text{Ba}_3\text{C}_{60}$  are quantitatively very similar to each other although the lattice constant of  $\text{K}_3\text{Ba}_3\text{C}_{60}$  is smaller than that of  $\text{Rb}_3\text{Ba}_3\text{C}_{60}$ . The  $t_{1g}$ -band, widths which are found to be equivalent to their widths at the N point, are 0.668 and 0.662 eV for  $\text{K}_3\text{Ba}_3\text{C}_{60}$  and  $\text{Rb}_3\text{Ba}_3\text{C}_{60}$ , respectively. We have found that the DOS profiles obtained for  $\text{K}_3\text{Ba}_3\text{C}_{60}$  and  $\text{Rb}_3\text{Ba}_3\text{C}_{60}$  are very similar to each other as expected from their similar band structure. Although the highest peak in the  $t_{1g}$ -band DOS of  $\text{K}_3\text{Ba}_3\text{C}_{60}$  is smaller than that of  $\text{Rb}_3\text{Ba}_3\text{C}_{60}$ , the Fermi level lies well above these peaks in both  $\text{K}_3\text{Ba}_3\text{C}_{60}$  and  $\text{Rb}_3\text{Ba}_3\text{C}_{60}$  and  $N(E_F)$  of  $\text{K}_3\text{Ba}_3\text{C}_{60}$  is slightly larger than that of  $\text{Rb}_3\text{Ba}_3\text{C}_{60}$ . Their  $N(E_F)$  values are 11.4 and 11.2 (states/eV  $\text{C}_{60}$  spins) for  $\text{K}_3\text{Ba}_3\text{C}_{60}$  and  $\text{Rb}_3\text{Ba}_3\text{C}_{60}$ , respectively. This  $N(E_F)$  value for  $\text{K}_3\text{Ba}_3\text{C}_{60}$  agrees very well with the experimental value of 11.4 (states/eV  $\text{C}_{60}$  spins) obtained from the measured Pauli paramagnetic susceptibility ( $\chi_s$ ) via  $N(E_F) = \chi_s / \mu_B^2$ .<sup>15</sup> On the other hand, the experimental value of  $N(E_F)$  for  $\text{Rb}_3\text{Ba}_3\text{C}_{60}$  (8.4 states/eV  $\text{C}_{60}$  spins) is smaller than the calculated value. The reason for this discrepancy for  $\text{Rb}_3\text{Ba}_3\text{C}_{60}$  is not clear yet. If other factors which can affect  $T_c$  besides  $N(E_F)$  are assumed to be identical in these two fullerides, a rather small difference in the calculated values of  $N(E_F)$  for  $\text{K}_3\text{Ba}_3\text{C}_{60}$  and  $\text{Rb}_3\text{Ba}_3\text{C}_{60}$  alone might not be enough to explain the difference in the experimental  $T_c$  values of these two fullerides. Regarding this point, we will discuss the isotope-effect-like mechanism later in this section.

The qualitative dispersion feature of three branches of the  $t_{1g}$  band in  $\text{K}_3\text{Ba}_3\text{C}_{60}$  is found to be essentially the same as

that in  $\text{K}_6\text{C}_{60}$  (Ref. 29) and  $\text{Ba}_6\text{C}_{60}$ .<sup>18,19</sup> Therefore,  $\text{K}_{3+x}\text{Ba}_{3-x}\text{C}_{60}$  ( $-3 \leq x \leq 3$ ) is expected to have also the similar  $t_{1g}$ -band dispersion, and consequently, the similar DOS profiles around the  $t_{1g}$ -band energy region. Because the number of valence electrons of  $\text{K}_{3+x}\text{Ba}_{3-x}\text{C}_{60}$  for  $x > 0$  is smaller than  $\text{K}_3\text{Ba}_3\text{C}_{60}$ , its Fermi level will eventually hit the DOS peak, which is estimated to take place at about  $x = 0.5$ . Hence,  $\text{K}_{3.5}\text{Ba}_{2.5}\text{C}_{60}$  may have higher  $T_c$  than  $\text{K}_3\text{Ba}_3\text{C}_{60}$ , if strength of electron-phonon coupling is comparable among  $\text{K}_{3+x}\text{Ba}_{3-x}\text{C}_{60}$  fullerides.

Next, in order to study the hybridization behavior more quantitatively, we have calculated  $t_{1g}$ -band widths at N point for several hypothetical bcc fullerides with the fixed lattice constant of  $a = 11.246$  or  $11.32$  Å. Systems studied are  $\text{Ba}_3\text{C}_{60}$  where K (or Rb) atoms are removed from  $\text{K}_3\text{Ba}_3\text{C}_{60}$  ( $\text{Rb}_3\text{Ba}_3\text{C}_{60}$ ), and  $\text{K}_6\text{C}_{60}$  with above  $a$  values. The atomic coordinates of  $\text{K}_6\text{C}_{60}$  assumed are identical to those of  $\text{K}_3\text{Ba}_3\text{C}_{60}$  for  $a = 11.246$  Å, and to those optimized in  $\text{Rb}_3\text{Ba}_3\text{C}_{60}$  for  $a = 11.32$  Å. In addition, the pristine bcc  $\text{C}_{60}$  with  $a = 11.32$  Å is also studied. Results are shown in the left and center column of Fig. 4.

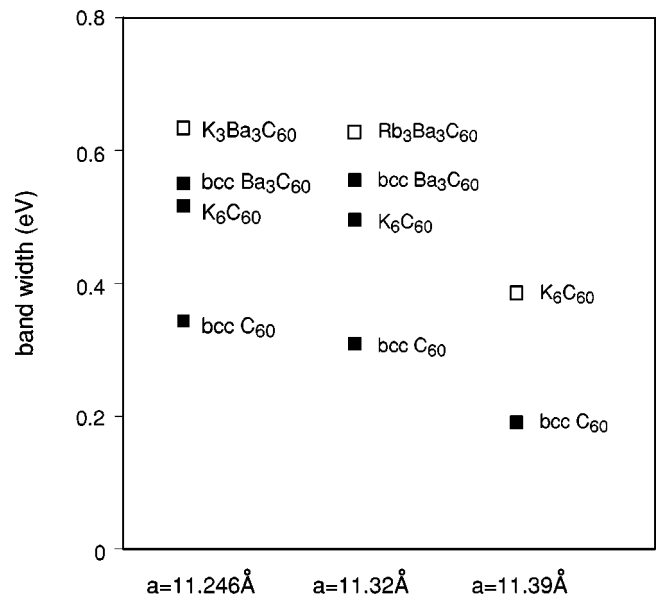


FIG. 4.  $t_{1g}$ -band widths of several fullerides. Fullerides denoted by filled boxes are hypothetical materials, while those by open boxes are real materials.

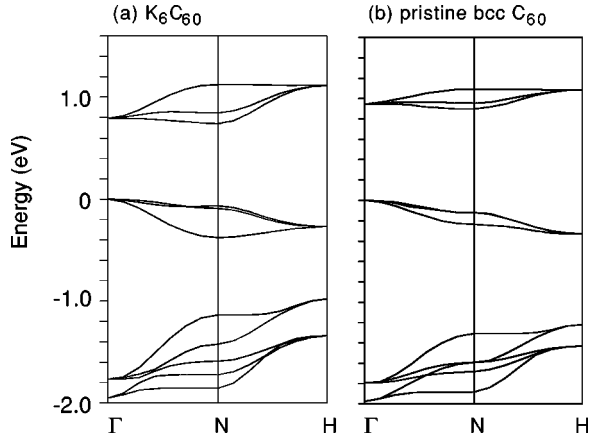


FIG. 5. Band structure of (a)  $K_6C_{60}$  and (b) the pristine bcc  $C_{60}$  at the same lattice constant  $a = 11.39$  Å. Energy is measured from  $t_{1u}$  states at the  $\Gamma$  point, i.e., the valence-band top in  $K_6C_{60}$ .

A considerable difference of 0.08 eV in  $t_{1g}$ -band widths of  $K_3Ba_3C_{60}$  and bcc  $Ba_3C_{60}$  at  $a = 11.246$  Å indicates the presence of the hybridization between K and  $C_{60}$  states in the  $K_3Ba_3C_{60}$  superconductor. Also, the difference of 0.21 eV in  $t_{1g}$ -band widths of bcc  $Ba_3C_{60}$  and bcc  $C_{60}$  at  $a = 11.246$  Å indicates the presence of the hybridization between Ba and  $C_{60}$  states. Similarly, the difference of 0.07 eV in  $t_{1g}$ -band widths of  $Rb_3Ba_3C_{60}$  and  $Ba_3C_{60}$  at  $a = 11.32$  Å has been obtained, indicating the presence of the hybridization between Rb and  $C_{60}$  states. For the bcc  $K_6C_{60}$ , the  $t_{1g}$ -band width at  $a = 11.246$  Å is slightly wider by 0.02 eV than that at  $a = 11.32$  Å. However, for  $Ba_3C_{60}$ , that at  $a = 11.246$  Å is almost identical to that at  $a = 11.32$  Å. Of course, the distance between the K (Ba) atom and its nearest C atom at  $a = 11.246$  Å is longer than that at  $a = 11.32$  Å. This indicates that, if the hybridization exists, the lattice-constant shortening does not always result in the simple broadening of the band structure. Therefore, the hybridization may be one of reasons for the complicated  $T_c$  behavior in  $A_3Ba_3C_{60}$ .

The hybridization between  $C_{60}$  states and alkali states in bcc fullerides has not been expected to take place so far.<sup>29</sup> Thus, in addition to  $A_3Ba_3C_{60}$ , we have calculated the magnitude of  $t_{1g}$ -band widths for the actual  $K_6C_{60}$  ( $a = 11.39$  Å) (Ref. 30) and the pristine  $C_{60}$  with the same

lattice constant. Results are shown in the right column of Fig. 4. The magnitude of the  $t_{1g}$ -band width at the  $N$  point for  $K_6C_{60}$  we have obtained is very similar to that of the previous calculation.<sup>29</sup> The band broadening due to the hybridization between K and  $C_{60}$  states are more clearly shown in Fig. 5 in which their band structure is given. It is evident that K-doping makes both  $t_{1g}$  and  $t_{1u}$  bands more dispersive.

There may be three possible reasons for the difference in the hybridization behaviors of bcc and fcc fullerides. First, they are different in their carbon-atom density. Because the fcc lattice is one of close-packed lattices,  $t_{1u}$  and  $t_{1g}$  states in the pristine fcc  $C_{60}$  should be densely distributed and the conduction channel via  $t_{1u}$  and  $t_{1g}$  states may be already developed well even in the pristine phase. Then, it may be unlikely for doped alkali atoms at interstitial sites to open new conduction channels. On the other hand, because in the bcc structure the carbon-atom density is smaller, there may still remain additional conduction channels to be opened by doping. Secondly, neighboring  $C_{60}$  clusters face to each other in a different way in bcc and fcc fullerides. In fcc fullerides, neighboring  $C_{60}$  clusters face to each other via pentagons. On the other hand, in bcc fullerides, neighboring  $C_{60}$  clusters face to each other via hexagons. As will be shown later, the  $t_{1g}$  state as well as the  $t_{1u}$  state has its amplitude more on pentagons than on hexagons. Therefore, in the bcc pristine  $C_{60}$ , both  $t_{1u}$  and  $t_{1g}$  bands should be narrow, while in the fcc pristine  $C_{60}$ , both  $t_{1u}$  and  $t_{1g}$  bands should be much wider. Actually,  $t_{1u}$  and  $t_{1g}$ -band widths of bcc pristine  $C_{60}$  ( $a = 11.246$  Å) are 0.23 and 0.34 eV, respectively, while those of fcc ( $a = 13.879$  Å) are both about 0.5 eV.<sup>31</sup> Thirdly,  $C_{60}$  clusters surrounding doped interstitial-site atoms show different faces towards doped atoms. In fcc fullerides,  $C_{60}$  clusters show hexagons toward tetrahedral interstitial sites and show hexagon-hexagon edge bonds toward octahedral interstitial sites, respectively. On the other hand, in bcc fullerides, each doped atom is surrounded by two pentagons and two hexagons. Therefore,  $t_{1u}$  and  $t_{1g}$  states can be easily hybridized with alkali states in bcc fullerides via pentagons.

Figure 6 shows the distribution of  $t_{1g}$  states,  $\rho_{t_{1g}}$ , on the (100) plane in the bcc pristine  $C_{60}$  and  $K_3Ba_3C_{60}$  with  $a = 11.246$  Å. The distribution  $\rho_{t_{1g}}$  is given by

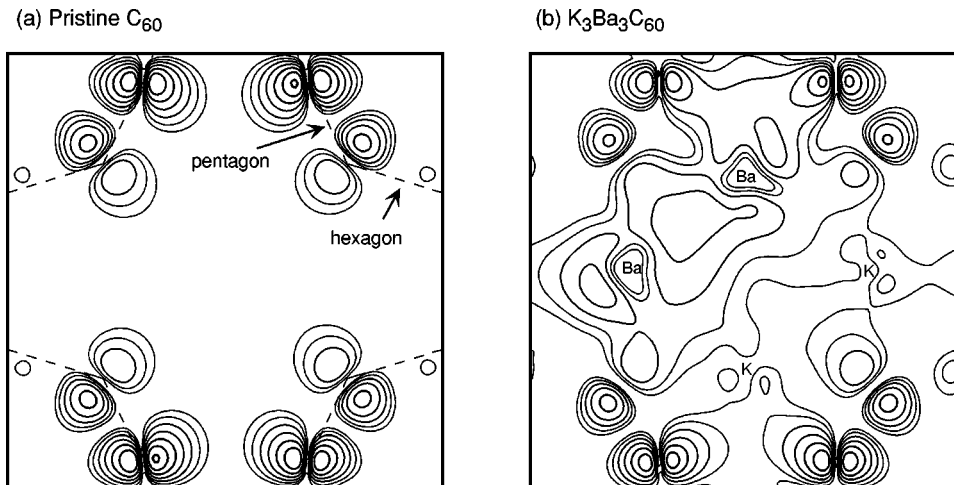


FIG. 6. Distribution of  $t_{1g}$  states on the (100) plane of (a) the bcc pristine  $C_{60}$  and (b)  $K_3Ba_3C_{60}$  at  $a = 11.246$  Å. Each contour line indicates twice (half) the density of the neighboring thinner (thicker) contour lines.

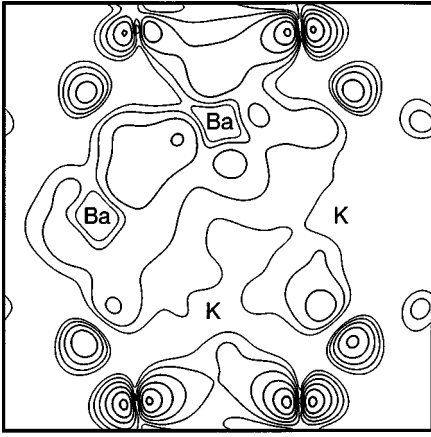


FIG. 7. Distribution of the states near the Fermi level on the (100) plane of  $K_3Ba_3C_{60}$ . Each contour line indicates twice (half) the density of the neighboring thinner (thicker) contour lines. Although the highest-density contours appear around C atoms, considerable amounts of  $\rho_{E_F}$  are observed also around K and Ba sites.

$$\rho_{t_{1g}}(\mathbf{r}) = \sum_n \int d\mathbf{k} \int dE |\Psi_{n\mathbf{k}}|^2 \delta(E - \epsilon_{n\mathbf{k}}).$$

Here, the energy integration is done in the energy range including only  $t_{1g}$  states and the same sampling points as used in the self-consistent calculation are taken for the  $\mathbf{k}$  integration. Figure 6 clearly indicates that  $t_{1g}$  states are spatially distributed more on pentagons than on hexagons in the bcc pristine  $C_{60}$  and that they are hybridized with alkali and Ba states in  $K_3Ba_3C_{60}$ .

In Fig. 7, the distribution of the states near the Fermi level,  $\rho_{E_F}$ ,

$$\rho_{E_F}(\mathbf{r}) = \sum_n \int d\mathbf{k} \int_{E_F - \Delta}^{E_F + \Delta} dE |\Psi_{n\mathbf{k}}|^2 \delta(E - \epsilon_{n\mathbf{k}}).$$

on the (100) plane in  $K_3Ba_3C_{60}$  is shown. Here  $\Delta = 0.1$  eV, which is the typical phonon energy in fullerenes, is used. Figure 7 indicates that the superconducting carriers should be on  $C_{60}$  clusters, around Ba sites, and around K sites. Hence, the carriers may be coupled not only with  $C_{60}$  intracluster phonons but also with the optical phonons involving Ba and K-ion displacements. The hybridization between  $C_{60}$  and K states therefore should play an important role in the superconductivity. We have also calculated  $\rho_{E_F}$  of  $Rb_3Ba_3C_{60}$ , which is confirmed to be very similar to that of

$K_3Ba_3C_{60}$ . Therefore, one of the reasons why  $T_c$  of  $K_3Ba_3C_{60}$  is higher than that of  $Rb_3Ba_3C_{60}$  may be the mass difference between K and Rb causing the  $T_c$  difference due to the effect similar to the isotope effect.

If this isotope-effect-like mechanism would be the case,  $Na_3Ba_3C_{60}$ , which has been not synthesized yet, might have higher  $T_c$  than that of  $K_3Ba_3C_{60}$ , because the Na atom is much lighter than the K atom. From the total-energy calculation, we have estimated the lattice constant of  $Na_3Ba_3C_{60}$ , which is found to be 11.09 Å. At this lattice constant,  $N(E_F)$  of  $Na_3Ba_3C_{60}$  obtained is 10.8 (states/eV), which is slightly smaller than that of  $K_3Ba_3C_{60}$  and less preferable for the superconductivity. Thus, whether  $Na_3Ba_3C_{60}$  has higher  $T_c$  than  $K_3Ba_3C_{60}$  or not is an open question.

#### IV. SUMMARY

We have studied the electronic structure of  $A_3Ba_3C_{60}$  ( $A = K$  or Rb) by using the local density approximation (LDA) within the framework of the density functional theory. It has been found that  $C_{60}$  states are hybridized with not only Ba states but also A states and the  $t_{1g}$ -derived band is half filled. The band-structure profiles of  $K_3Ba_3C_{60}$  and  $Rb_3Ba_3C_{60}$  are very similar to each other and the density of states at the Fermi level of  $K_3Ba_3C_{60}$  is slightly higher than that of  $Rb_3Ba_3C_{60}$ , although the lattice constant of  $K_3Ba_3C_{60}$  is smaller than that of  $Rb_3Ba_3C_{60}$ . Carriers to be responsible for the superconductivity is found to be not only on  $C_{60}$  clusters and around Ba atoms but also around K (Rb) atoms. Therefore, the hybridization between  $C_{60}$  and K (Rb) states as well as between  $C_{60}$  and Ba states should play an important role in their electronic properties including the superconductivity. This novel hybridization between  $C_{60}$  and K states is found to take place in  $K_6C_{60}$  as well.

#### ACKNOWLEDGMENTS

We would like to thank Professor Y. Iwasa for providing his results prior to publication. Numerical calculations were performed on a Fujitsu VPP500 at the Institute for Solid State Physics, University of Tokyo, a Fujitsu VPP700 at Kyushu University, and an NEC SX3/34R at the Institute for Molecular Science, Okazaki National Institute. This work was supported by a Grant-in-Aid for Scientific Research on the Priority Area "Fullerenes and Nanotubes" by the Ministry of Education, Science, and Culture of Japan, the Nissan Science Foundation, and the Japan Society for the Promotion of Science (Project No. 96P00203).

<sup>1</sup>A.F. Hebard, M.J. Rosseinsky, R.C. Haddon, D.W. Murphy, S.H. Glarum, T.T.M. Palstra, A.P. Ramirez, and A.R. Kortan, *Nature (London)* **350**, 600 (1991).

<sup>2</sup>P.W. Stephens, L. Mihaly, P.L. Lee, R.L. Whetten, S.M. Huang, R. Kaner, F. Deiderich, and K. Holczer, *Nature (London)* **351**, 632 (1991).

<sup>3</sup>K. Tanigaki, I. Hirose, T.W. Ebbesen, J. Mizuki, and J.S. Tsai, *J. Phys. Chem. Solids* **54**, 1645 (1993), and references therein.

<sup>4</sup>M.J. Rosseinsky, A.P. Ramirez, S.H. Glarum, D.W. Murphy, R.C. Haddon, A.F. Hebard, T.T.M. Palstra, A.R. Kortan, S.M.

Zahurak, and A.V. Makhija, *Phys. Rev. Lett.* **66**, 2830 (1991).

<sup>5</sup>K. Holczer, O. Klein, S.M. Huang, R.B. Kaner, K.J. Fu, R.L. Whetten, and F. Diederich, *Science* **252**, 1154 (1991).

<sup>6</sup>K. Tanigaki, T.W. Ebbesen, S. Saito, J. Mizuki, J.S. Tsai, Y. Kubo, and S. Kuroshima, *Nature (London)* **352**, 222 (1991). Superconductivity at 40 K under pressure was reported in  $Cs_3C_{60}$  which is not the fcc fullerene [T.T.M. Palstra, O. Zhou, Y. Iwasa, P.E. Sulewski, R.M. Fleming, and B.R. Zegarski, *Solid State Commun.* **93**, 327 (1995)].

<sup>7</sup>S. Saito and A. Oshiyama, *Phys. Rev. B* **44**, 11 536 (1991).

- <sup>8</sup>M. Schluter, M. Lannoo, M. Needels, G.A. Baraff, and D. Tománek, *Phys. Rev. Lett.* **68**, 526 (1992).
- <sup>9</sup>C.M. Varma, J. Zaanen, and K. Raghavachari, *Science* **254**, 989 (1991).
- <sup>10</sup>J.L. Martins and N. Troullier, *Phys. Rev. B* **46**, 1766 (1992).
- <sup>11</sup>A. Oshiyama and S. Saito, *Solid State Commun.* **82**, 41 (1992).
- <sup>12</sup>G. Sparr, J.D. Thompson, R.L. Whetten, S.M. Huang, R.B. Kaner, F. Diederich, G. Grüner, and K. Holczer, *Phys. Rev. Lett.* **68**, 1228 (1992).
- <sup>13</sup>Y. Iwasa, H. Hayashi, T. Furudate, and T. Mitani, *Phys. Rev. B* **54**, 14 960 (1996).
- <sup>14</sup>T. Takenobu, S. Taga, M. Kawaguchi, Y. Iwasa, and T. Mitani, in *Meeting Abstracts of the Physical Society of Japan*, (Physical Society of Japan, Tokyo, 1997), vol. 52, Issue 2, Pt. 2, p. 281.
- <sup>15</sup>Y. Iwasa, M. Kawaguchi, H. Iwasaki, T. Mitani, N. Wada, and T. Hasegawa, *Phys. Rev. B* **57**, 13 395 (1998).
- <sup>16</sup>A.R. Kortan, N. Kopylov, S. Glarum, E.M. Gyorgy, A.P. Ramirez, R.M. Fleming, O. Zhou, F.A. Thiel, P.L. Trevor, and R.C. Haddon, *Nature (London)* **360**, 566 (1992).
- <sup>17</sup>A.R. Kortan, N. Kopylov, E. Ozdas, A.P. Ramirez, R.M. Fleming, and R.C. Haddon, *Chem. Phys. Lett.* **243**, 501 (1994).
- <sup>18</sup>S. Saito and A. Oshiyama, *Phys. Rev. Lett.* **71**, 121 (1993).
- <sup>19</sup>S. Saito and A. Oshiyama, *J. Phys. Chem. Solids* **54**, 1759 (1993).
- <sup>20</sup>B. Gogia, K. Kordatos, H. Suematsu, K. Tanigaki, and K. Prasad, *Phys. Rev. B* **58**, 1077 (1998).
- <sup>21</sup>P. Hohenberg and W. Kohn, *Phys. Rev.* **136**, B864 (1964).
- <sup>22</sup>W. Kohn and L.J. Sham, *Phys. Rev.* **140**, A1133 (1965).
- <sup>23</sup>J.P. Perdew and A. Zunger, *Phys. Rev. B* **23**, 5048 (1981); D.M. Ceperley and B.J. Alder, *Phys. Rev. Lett.* **45**, 566 (1980).
- <sup>24</sup>N. Troullier and J.L. Martins, *Phys. Rev. B* **43**, 1993 (1990).
- <sup>25</sup>L. Kleinman and D.M. Bylander, *Phys. Rev. Lett.* **48**, 1425 (1982).
- <sup>26</sup>M. Saito, O. Sugino, and A. Oshiyama, *Phys. Rev. B* **46**, 2606 (1992).
- <sup>27</sup>O. Sugino and A. Oshiyama, *Phys. Rev. Lett.* **68**, 1858 (1992).
- <sup>28</sup>S.G. Louie, S. Froyen, and M.L. Cohen, *Phys. Rev. B* **26**, 1738 (1982).
- <sup>29</sup>S.C. Erwin and M.R. Pederson, *Phys. Rev. Lett.* **67**, 1610 (1991).
- <sup>30</sup>O. Zhou, J.E. Fisher, N. Coustel, S. Kycia, Q. Zhu, A.R. McGhie, W.J. Romanow, J.P. McCauley, Jr., A.B. Smith III, and D.E. Cox, *Nature (London)* **351**, 462 (1991).
- <sup>31</sup>N. Troullier and J.L. Martins, *Phys. Rev. B* **46**, 1754 (1992).